rings are listed in Table 2. Their two mean planes form an angle of 7·3°. The phenyl ring is planar ($\chi^2 = 10·2$), as is the five-membered furyl ring ($\chi^2 = 7·4$).

The Br^- is involved in two hydrogen bonds, one to $N^+(4)$ of the main molecule and the other to O(27) of the solvent (Fig. 3). The corresponding dimensions are: Br···H(4) 2·50, Br···N(4) 3·31 Å, Br···H(4)–N(4) 175°; Br···H(27) 2·26, Br···O(27) 3·22 Å, Br···H(27)–O(27) 159°. There are no other short intermolecular contacts.

The authors thank Professor R. T. LaLonde of the State University of New York at Syracuse for the crystal samples, and Mrs M. E. Pippy for assistance with the computations.

References

AHMED, F. R., HALL, S. R., PIPPY, M. E. & HUBER, C. P. (1973). NRC Crystallographic Programs for the IBM 360 System. Accession Nos. 133–147, *J. Appl. Cryst.* **6**, 309–346.

HANSON, H. P., HERMAN, F., LEA, J. D. & SKILLMAN, S. (1964). *Acta Cryst.* **17**, 1040–1044.

LALONDE, R. T., TSAI, A. I.-M. & WONG, C. F. (1976). *J. Org. Chem.* **41**, 2514–2520.

STEWART, R. F., DAVIDSON, E. R. & SIMPSON, W. T. (1965). *J. Chem. Phys.* **42**, 3175–3187.

Acta Cryst. (1977). B**33**, 466–472

An Electron Density Study of $NaCN.2H_2O$ at 150 K

BY J. W. BATS*

Chemistry Department, State University of New York, Buffalo, New York 14214, *USA*

(*Received* 6 *April* 1976; *accepted* 19 *July* 1976)

The crystal structure of $NaCN.2H_2O$ has been refined from X-ray data measured at 150 K on a four-circle diffractometer. The CN group is found to be inverted compared with a previously reported study [LeBihan, *Acta Cryst.* (1958), **11**, 770–773]. The cyanide group is bonded mainly through the N atom to the Na atom, while the C atom is involved in two hydrogen bonds with hydrate molecules. Results of an all-data refinement and a high-order refinement are compared. Considerable lone-pair density is observed at the back of the C atom in the deformation maps. Analyses of the charge distribution show a net charge on the CN group of −0·50 e. The Na atom is almost neutral, while the positive charge in the crystal is concentrated on the hydrate molecules.

Introduction

The crystal structure of $NaCN.2H_2O$ was first determined by LeBihan (1958) and it was concluded that, in contrast to many simple cyanides where the CN group is disordered, an ordered CN group is present in $NaCN.2H_2O$ as a result of interactions of this group with hydrogen bonds.

Determination of the electron density seemed of considerable interest, because the cyanide ion is small and can be relatively easily studied theoretically, and because of the insight into the nature of the water molecule binding in crystalline hydrates that may be obtained. It was therefore decided to undertake an accurate redetermination of its structure. In order to reduce thermal motion the study was performed at reduced temperature.

Experimental

Single crystals of $NaCN.2H_2O$ were grown from an aqueous solution of NaCN. A crystal of approximately 0·30 × 0·30 × 0·35 mm was selected for data collection and sealed in a glass capillary as the crystals rapidly decomposed in the air. The crystal was cooled with a stream of cold nitrogen gas. A temperature of 150 K was chosen for the experiment. Below this temperature ice formation became a serious problem. The space group $P2_1/c$, reported earlier (LeBihan, 1958), was confirmed. Crystallographic information is repor-

* Present address: Chemical Physics Laboratory, Twente University of Technology, PO Box 217, Enschede, The Netherlands.

Table 1. *General information*

$a = 5{\cdot}968\ (2)$ Å	Crystal volume	0·033 mm³
$b = 10{\cdot}508\ (4)$	Wavelength	0·71069 Å
$c = 6{\cdot}572\ (2)$	$(\sin\theta/\lambda)_{max}$	0·92 Å^{-1}
$\beta = 102{\cdot}07\ (2)°$	Number of reflections	6729
$V = 403{\cdot}03\ (24)$ Å³	Unique reflections	2701
Space group $P2_1/c$	μ	2·25 cm^{-1}
	Transmission range	0·923–0·957

ted in Table 1. Step-scan data were collected in three quadrants of the reciprocal space up to sin θ/λ values of 0·92, 0·91 and 0·65 Å^{-1} respectively on a Picker FACS-I diffractometer with Nb-filtered Mo $K\alpha$ radiation (Blessing, Coppens & Becker, 1974). Three standard reflections were measured after every 50 reflections and all data rescaled with respect to these standards; the maximum fluctuation of the standards was about 1%. The data were corrected for Lorentz, polarization and absorption effects, while deviations from the counter linearity were corrected using the method of Chipman (1969). Related reflections were averaged ($\Sigma|F^2 - \langle F^2\rangle|/\Sigma F^2 = 1{\cdot}8\%$), resulting in 2484 independent reflections with larger than zero net intensity. A weighting scheme was assigned to the final data set according to $w(F^2) = [\sigma(F^2)_{counting} + kF^2]^{-2}$ with $k = 0{\cdot}01$ derived from the variations in symmetry-related reflections.

Structure refinement

Initial positional parameters for the non-hydrogen atoms were taken from LeBihan (1958). A least-squares refinement with isotropic thermal parameters gave unrealistic thermal parameters for the atoms of the cyanide group (C atom $B = 1{\cdot}0$, N atom $B = 2{\cdot}8$), indicating that the two atoms had to be reversed. This lowered the value of R from 11 to 7%, and changed the thermal parameters of the C and N atoms to comparable values. A difference Fourier synthesis indicated the positions of all four H atoms. Scattering factors for the non-hydrogen atoms were taken from *International Tables for X-ray Crystallography* (1974), and those for the H atoms from Stewart, Davidson & Simpson (1965). For the Na atom the anomalous scattering factors of Cromer & Liberman (1970) were applied. Extinction was found to be negligible.

As atomic parameters obtained from a conventional X-ray refinement are known to be biased by bonding effects, an additional least-squares refinement was done on only the high-order reflections with sin $\theta/\lambda > 0{\cdot}65$ Å^{-1}. In this high-order refinement, the atomic parameters of the H atoms were not varied. Details about the least-squares refinements are given in Table 2. The positional and thermal parameters from the conventional and high-order refinement are given in Table

Table 2. *Review of least-squares refinements*

	Conventional	High order
$(\sin\theta/\lambda)_{min}$ (Å^{-1})	0·00	0·65
$(\sin\theta/\lambda)_{max}$ (Å^{-1})	0·92	0·92
Number of reflections	2484	1577
Number of variables	62	46
Scale factor	8·272 (9)	8·162 (41)
$R(F)$(%)	4·3	7·6
$R_w(F)$(%)	2·9	3·8
Goodness of fit*	1·71	0·97

* Defined as: $[\Sigma w(|F_o| - |F_c|)^2/(NO - NV)]^{\frac{1}{2}}$.

Table 3. *Positional* ($\times 10^5$; *for* H $\times 10^4$) *and thermal* ($\times 10^4$; *for* H $\times 10^3$) *parameters*

The temperature factor is defined as: $\exp[-2\pi^2(h^2a^{*2}U_{11} + 2hka^*b^*U_{12} + \cdots)]$.

Conventional refinement

	x	y	z	U_{11}	U_{22}	U_{33}	U_{12}	U_{13}	U_{23}
Na	103 (4)	17050 (2)	93587 (3)	217 (1)	156 (1)	186 (1)	−15 (1)	25 (1)	−11 (1)
O(1)	74424 (7)	29802 (4)	67779 (7)	225 (2)	179 (2)	261 (2)	−1 (2)	43 (2)	−4 (2)
O(2)	19699 (7)	47913 (4)	69094 (7)	189 (2)	207 (2)	195 (2)	−15 (1)	6 (1)	30 (2)
N	23294 (9)	15627 (5)	61986 (9)	305 (3)	232 (2)	259 (2)	53 (2)	56 (2)	19 (2)
C	31965 (10)	6817 (6)	70023 (9)	243 (3)	245 (3)	240 (3)	48 (2)	68 (2)	18 (2)

	x	y	z	U		x	y	z	U
H(1)	7151 (15)	3733 (10)	7142 (14)	50 (3)	H(3)	3301 (16)	4898 (8)	6991 (13)	40 (2)
H(2)	6152 (17)	2613 (11)	6430 (17)	63 (3)	H(4)	1862 (15)	4555 (9)	7973 (15)	49 (3)

High-order refinement

	x	y	z	U_{11}	U_{22}	U_{33}	U_{12}	U_{13}	U_{23}
Na	100 (6)	17047 (3)	93585 (6)	212 (2)	153 (1)	183 (2)	−14 (1)	26 (1)	−10 (1)
O(1)	74371 (10)	29810 (6)	67779 (11)	220 (2)	178 (2)	255 (2)	0 (1)	44 (2)	0 (2)
O(2)	19734 (10)	47903 (5)	69162 (9)	188 (2)	197 (2)	193 (2)	−10 (1)	2 (1)	26 (2)
N	23185 (15)	15658 (7)	61942 (13)	304 (3)	214 (3)	260 (3)	70 (2)	45 (2)	35 (2)
C	31997 (14)	6762 (8)	70045 (13)	250 (3)	225 (3)	249 (3)	68 (2)	61 (2)	42 (2)

3.* The programs used for data reduction and structure refinement are part of the Integrated Crystallographic Computing Library at the State University of New York at Buffalo.

Discussion of the structure

The main bond lengths and angles in $NaCN.2H_2O$ are given in Table 4. Fig. 1 shows a stereoscopic view of the atomic arrangement.

As the present structure determination of $NaCN.2H_2O$ gives considerably different results from those of the previous study (LeBihan, 1958) the structure is briefly described below.

Sodium is bonded to the cyanide group mainly *via* the N atom. A short Na–N contact is found almost parallel to the CN axis, while a second, somewhat longer Na–N interaction is found almost perpendicular to this axis.

The Na atom has a distorted octahedral coordination of four hydrate O atoms and two N atoms. All four O–Na contacts are in the lone-pair directions of sp^3-hybridized hydrate O atoms.

Four possible hydrogen bonds can be found and are reported in Table 5. Two are of type O–H···N with O···N distances of 3·120 and 3·347 Å and lie in a plane almost perpendicular to the CN axis through the N atom.

The two other interactions are of type O–H···C, with O···C distances of 2·969 and 2·989 Å. These latter hydrogen bonds are rather unusual. As X-ray positions of H atoms are generally shifted by about 0·10 to 0·20 Å towards the O atoms to which they are bonded, the H···C interatomic distances should be about 2·05 Å. This is considerably shorter than the sum of the van der Waals radii of the C and H atoms. Together with the approximate linearity of both O–H–C angles, this suggests that these interactions can be classified as hydrogen bonds.

* A list of structure factors has been deposited with the British Library Lending Division as Supplementary Publication No. SUP 32062 (15 pp.). Copies may be obtained through The Executive Secretary, International Union of Crystallography, 13 White Friars, Chester CH1 1NZ, England.

Table 4. *Bond lengths* (Å) *and angles* (°)

	Conventional refinement	High-order refinement
C–N	1·136 (1)	1·148 (1)
N–Na	2·448 (1)	2·442 (1)
N–Na′	2·730 (1)	2·728 (1)
C–Na′	2·899 (1)	2·901 (1)
O(1)–Na	2·436 (1)	2·438 (1)
O(1)–Na′	2·451 (1)	2·453 (1)
O(2)–Na	2·392 (1)	2·395 (1)
O(2)–Na′	2·415 (1)	2·417 (1)
O(1)–H(1)	0·85 (1)	—
O(1)–H(2)	0·85 (1)	—
O(2)–H(3)	0·79 (1)	—
O(2)–H(4)	0·76 (1)	—
C–N–Na	172·60 (5)	172·81 (8)
C–N–Na′	86·85 (4)	86·86 (7)
H(1)–O(1)–H(2)	105·6 (9)	—
H(3)–O(2)–H(4)	105·2 (8)	—

Table 5. *Hydrogen bonds* (X···H–O)

X···H–O	X···H (Å)	X···O (Å)	X–H–O (°)
N···H(2)–O(1)	2·51 (1)	3·347 (1)	168 (1)
N···H(4)–O(2)	2·39 (1)	3·120 (1)	165 (1)
C···H(1)–O(1)	2·14 (1)	2·989 (1)	173 (1)
C···H(3)–O(2)	2·21 (1)	2·969 (1)	160 (1)

Table 6. *Positional asphericity shifts* (Å) (*conventional – high order*)

Na	0·0004 (4)	O(1)	0·0033 (6)
C	0·0067 (9)	O(2)	0·0050 (6)
N	0·0084 (9)		

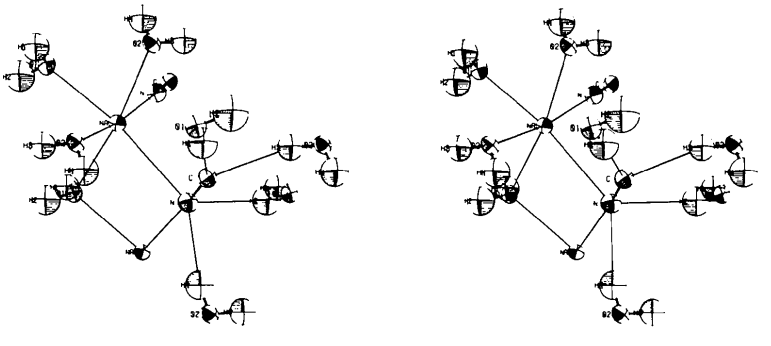

Fig. 1. Stereoscopic view of the structure. The thermal ellipsoids enclose 50% probability.

Analysis of the chemical bonding

The positional parameters of the C, N and O atoms from the conventional and high-order refinements differ significantly (Table 6). The C and N atoms are shifted in the CN bond by 0·007 and 0·008 Å in the conventional refinement, while atoms O(1) and O(2) are shifted in their lone-pair directions by 0·003 and 0·005 Å respectively. This is in general agreement with shifts observed in other compounds (Coppens, 1974); both the direction and magnitude of the shifts of the C and N atoms are similar to those observed in tetracyanoethylene (Little, Pautler & Coppens, 1971).

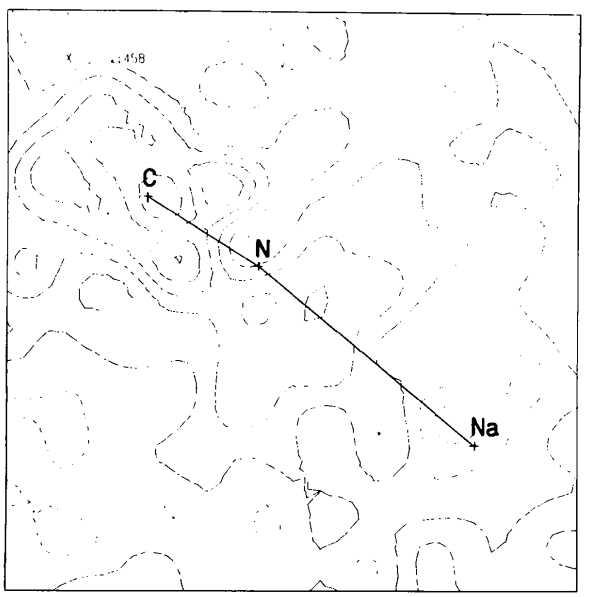

Fig. 2. Deformation density in section through NaNC group, after conventional X-ray refinement. Data cut-off in Fourier synthesis: $\sin\theta/\lambda = 0{\cdot}75$ Å^{-1}. Contour interval 0·05 e Å^{-3}; negative contours broken.

Figs. 2 and 3 show difference density maps in a plane through the NaNC group, with the atomic parameters taken from the conventional and high-order refinement respectively. The scale factor from the conventional refinement has been used in the calculation of the maps. The high-order scale factor is less accurate as a result of a larger correlation with the thermal parameters in the high-order refinement and is not significantly different from the conventional scale factor.

It is obvious from Fig. 2 that the atomic parameters from the conventional refinement are heavily biased by bonding effects as this map is almost featureless. Fig. 3 shows considerably more detail. The strong bond peak in the triply bonded cyanide group explains the shortening of the CN bond length in the conventional refinement. The strong carbon lone-pair density supports the existence of O—H · · · C hydrogen bonds.

The valence density, *i.e.* the observed electron density minus the core density of the free atoms in the NaNC section, is shown in Fig. 4. This map is dominated by the valence density of the C and N atoms and is therefore less illustrative in showing bonding features than the difference maps.

Fig. 5 shows the deformation density in a section through the midpoint of the CN bond, perpendicular to this bond. The shape of this triple bond peak is almost

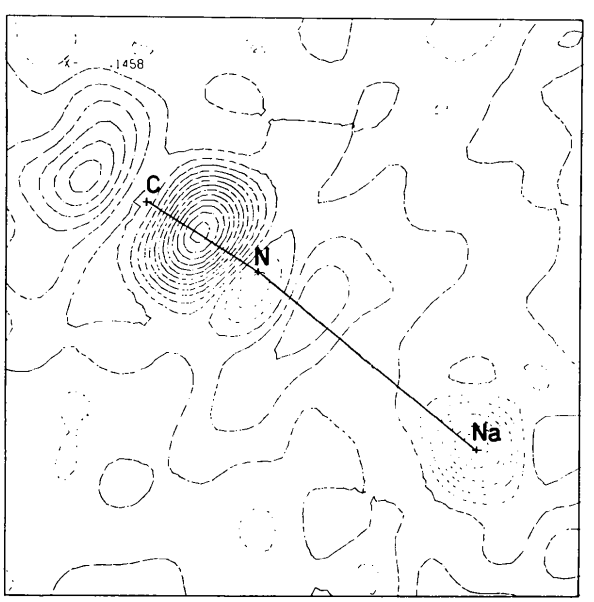

Fig. 3. Deformation density in section through NaNC group, after high-order X-ray refinement. Data cut-off and contour intervals as in Fig. 2.

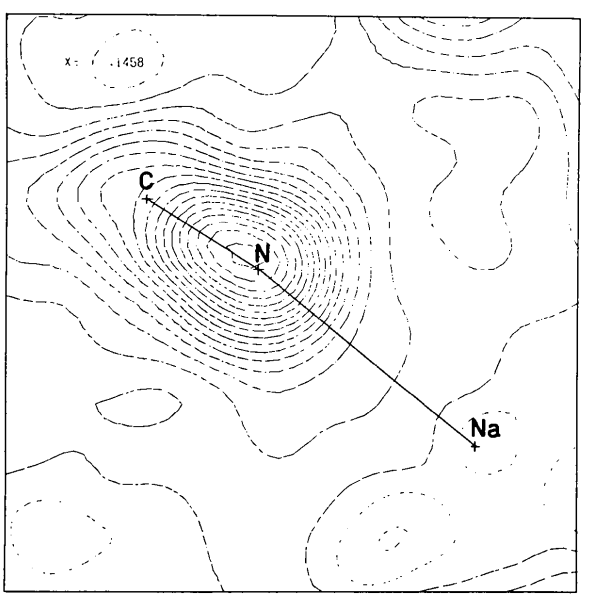

Fig. 4. Observed valence density in section through NaNC group. Data cut-off in Fourier synthesis: $\sin\theta/\lambda = 0{\cdot}75$ Å^{-1}. Contour interval 0·2 e Å^{-3}; negative contours broken.

cylindrical as has been observed elsewhere (C≡C: Helmholdt, 1975; C≡N: Becker, Coppens & Ross, 1973).

The experimental deformation density of the CN group shows good qualitative resemblance to the theoretical deformation density of CN^- calculated by Bats & Feil (1977) from the extended *ab initio* molecular wavefunctions of Bonaccorsi, Petrongolo, Scrocco & Tomasi (1969) and reproduced in Fig. 6. The experimental peak height in the CN bond is in good agreement with the theoretical value when the effect of thermal smearing as outlined by Becker, Coppens & Ross (1973) is taken into account. The N lone-pair peak is lower than expected; this may be because of a small contribution of bonding effects to the high-order reflections. Atomic parameters from an independent neutron diffraction experiment would be needed to justify this assumption. A detailed comparison of the experimental and dynamical-theoretical densities for the present and related compounds is presently in progress.

Figs. 7 and 8 show the deformation density in sections through the hydrate O atoms and the Na atoms. Both O atoms have excess density in their lone-pair region. The lone-pair features are however weak and

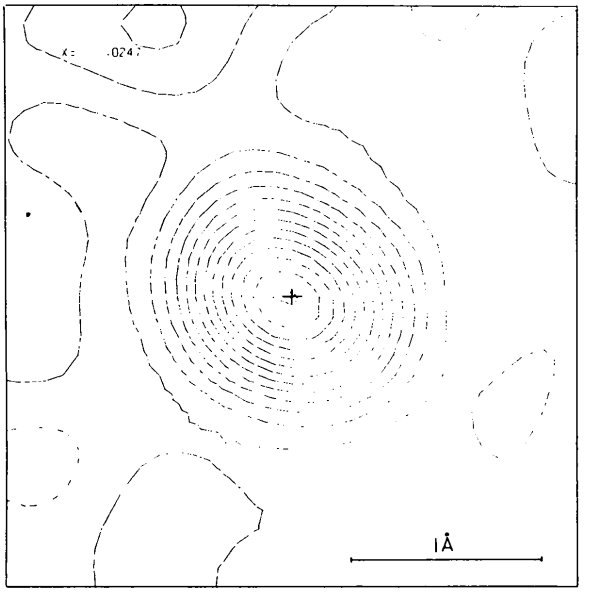

Fig. 5. Deformation density in cross-section through the CN bond, normal to the bond. Contours as in Fig. 2.

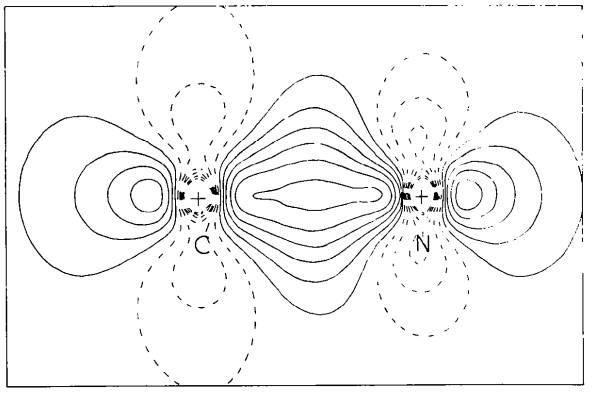

Fig. 6. Theoretical deformation density for CN^- after Bats & Feil (1977). Contour interval 0·025 e.a.u.$^{-3}$; negative and zero contours broken.

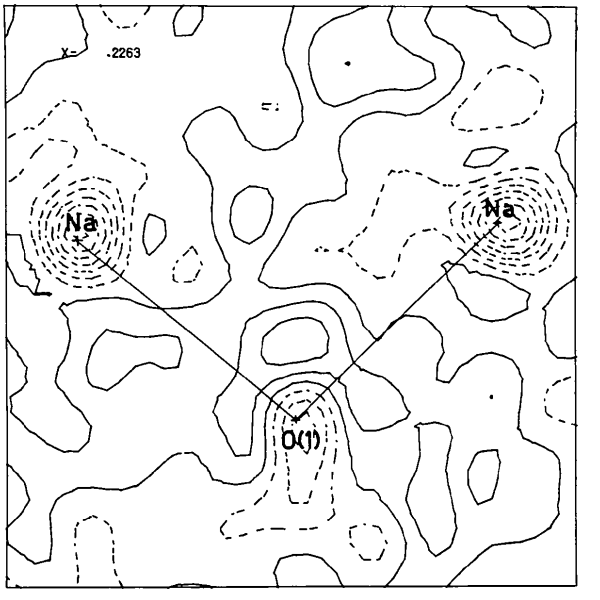

Fig. 7. Deformation density in section through O(1) and Na atoms. Contours as in Fig. 2.

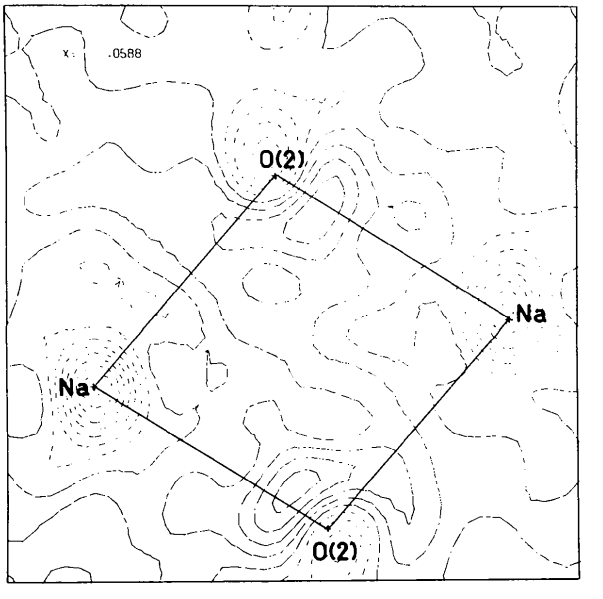

Fig. 8. Deformation density in section through O(2) and Na atoms. Contours as in Fig. 2.

not very well defined. This is not surprising as O lone-pair electrons are known to scatter beyond the $\sin\theta/\lambda$ limit of 0·65 Å^{-1}. The atomic parameters of the O atoms determined in the high-order refinement are therefore expected to compensate partly for the bonding effects in the lone pairs. An X–X (high order) map of *p*-nitropyridine *N*-oxide, for example, shows considerably less lone-pair density at the O atoms when the data cut-off is lowered from 0·75 to 0·65 Å^{-1} in $\sin\theta/\lambda$ (Wang, Blessing, Ross & Coppens, 1976; Coppens & Lehmann, 1976).

In order to obtain information on the net atomic charge on the atoms in $NaCN.2H_2O$, the valence-shell projection method described by Stewart (1970) has been applied to the present data set. Scattering factors for core and valence shells of the atoms were taken from Fukamachi (1971). It was found that the diffuse 3*s* orbital of Na gave an insufficient contribution to the total scattering to allow refinement of its electron population. Therefore, the population of this orbital was fixed to 1·0 and the population of the Na *L*-shell was varied instead. Refinements with and without a constraint for electroneutrality of the structure were found to give identical net atomic charges. The net atomic charges are given in Table 7.

Table 7. *Net atomic charges from valence-shell projection method*

Na	+0·10 (1)	H(1)	+0·14 (2)
C	−0·36 (3)	H(2)	+0·06 (2)
N	−0·11 (2)	H(3)	+0·09 (2)
O(1)	−0·08 (2)	H(4)	+0·16 (2)
O(2)	0·00 (2)		

Table 8. *Net charge on sodium atom determined by numerical integration*

Effective radius (Å)	Net charge	Volume of integration (Å^3)
0·90	+0·15 (7)	5·3
1·05	+0·16 (6)	7·2
1·20	+0·14 (6)	9·9
1·35	+0·10 (5)	12·9
1·50	+0·05 (4)	16·7
1·65	0·00 (3)	21·0
1·80	−0·06 (3)	26·1

Table 9. *Net charges on molecular fragments*

Group	Net charge (integration)	Net charge (projection)
Na	+0·05 (4)	+0·10 (1)
CN	−0·50 (3)	−0·47 (4)
H_2O(I)	+0·22 (3)	+0·12 (4)
H_2O(II)	+0·24 (2)	+0·25 (4)

A different way to determine net charges on atoms or groups of atoms is by a numerical integration over a three-dimensional Fourier synthesis as described by Coppens (1975). The molecular volume is defined by dividing the space between two neighboring atoms belonging to different molecules, according to the ratio of the van der Waals radii of these atoms. The van der Waals radii of C, N, O and H were taken as 1·4, 1·5, 1·4 and 1·2 Å.

The choice of a radius for the Na atom was less obvious so it was treated as a variable. As only shifts of charges interest us, the integration has been performed on the deformation density.

Table 8 lists the net charge on the Na atom as a function of the radius. It should be emphasized that the radius given in Table 8 is an effective radius assigned to the Na atom and does not correspond to the limit of integration. The standard deviation assigned to the observed net charges is derived from the errors in the observed structure factors and an error in the scale factor of 1%. The charges reported in Table 8 are not very dependent on the effective radius assigned to the Na atom. A radius for the Na atom of 1·5 Å will therefore be assumed in the following discussion.

Net charges for the ions and molecules obtained by integration are compared with values from the valence-shell projection method in Table 9.

The results of both methods are in good agreement, though the integration method can be considered more realistic than the projection method, as the spherical atomic valence shells used in the latter method are probably poor representations of the shape of the deformation density.

The cyanide ion bears a net charge of about −0·50 e. There is a charge transfer of about 0·23 e from both hydrate molecules, in good agreement with the average value of +0·18 e calculated by Coppens, Pautler & Griffin (1971) for four hydrate molecules with the extended *L*-shell projection method.

The net charge on the Na atom is almost zero, in agreement with the electroneutrality principle of Pauling (1948), which states that for hydrated cations the positive charge is transferred to the outermost H atoms of the complex.

Support of this work by the National Science Foundation is gratefully acknowledged.

References

BATS, J. W. & FEIL, D. (1977). To be published.

BECKER, P., COPPENS, P. & ROSS, F. K. (1973). *J. Amer. Chem. Soc.* **95**, 7604–7609.

BLESSING, R. H., COPPENS, P. & BECKER, P. (1974). *J. Appl. Cryst.* **7**, 488–492.

BONACCORSI, R., PETRONGOLO, C., SCROCCO, E. & TOMASI, J. (1969). *Chem. Phys. Lett.* **3**, 473–475.

CHIPMAN, D. R. (1969). *Acta Cryst.* A**25**, 209–213.
COPPENS, P. (1974). *Acta Cryst.* B**30**, 255–261.
COPPENS, P. (1975). *Phys. Rev. Lett.* **35**, 98–100.
COPPENS, P. & LEHMANN, M. S. (1976). *Acta Cryst.* B**32**, 1777–1784.
COPPENS, P., PAUTLER, D. & GRIFFIN, J. F. (1971). *J. Amer. Chem. Soc.* **93**, 1051–1058.
CROMER, D. T. & LIBERMAN, D. (1970). *J. Chem. Phys.* **53**, 1891–1898.
FUKAMACHI, T. (1971). Technical Report of Institute for Solid State Physics, Univ. of Tokyo, Series B12.
HELMHOLDT, R. B. (1975). Thesis, Univ. of Groningen.
International Tables for X-ray Crystallography (1974). Vol. IV. Birmingham: Kynoch Press.
LEBIHAN, M. T. (1958). *Acta Cryst.* **11**, 770–773.
LITTLE, R. G., PAUTLER, D. & COPPENS, P. (1971). *Acta Cryst.* B**27**, 1493–1499.
PAULING, L. (1948). *J. Chem. Soc.* pp. 1461–1467.
STEWART, R. F. (1970). *J. Chem. Phys.* **53**, 205–213.
STEWART, R. F., DAVIDSON, E. R. & SIMPSON, W. T. (1965). *J. Chem. Phys.* **42**, 3175–3187.
WANG, Y., BLESSING, R. H., ROSS, F. K. & COPPENS, P. (1976). *Acta Cryst.* B**32**, 572–578.

Acta Cryst. (1977). B**33**, 472–479

Structure and Binding in Molecular Complexes of Cyclic Polyethers. III.* Host–Guest Interaction Involving Two Assemblies of Binding Sites†

BY ISRAEL GOLDBERG

Department of Chemistry, Tel-Aviv University, Tel-Aviv, Israel

(*Received* 24 *May* 1976; *accepted* 18 *July* 1976)

The crystal structure of the one-to-one complex between a synthetic ligand (I) ($C_{40}H_{50}O_{12}$) containing two 18-crown-6 macrocyclic moieties and a bis(hexafluorophosphate) salt of tetramethylenediamine has been determined by X-ray diffraction methods at low temperature (−160°C). Crystals are orthorhombic, space group *Pbcn*, with $a = 18{\cdot}971\ (3)$, $b = 19{\cdot}137\ (3)$, $c = 13{\cdot}932\ (2)$ Å, and $Z = 4$. The structure was solved by direct methods and refined by full-matrix least-squares methods to $R = 0{\cdot}059$ for 2371 independent reflexions measured by counter diffractometry. In the solid, the molecules are located on crystallographic twofold axes. The macro-ring assemblies of binding sites in the host are held in a convergent relationship through hydrogen bonding to functional groups of the guest species. The ammonium ions centre into the inside faces of the macrocycles, the tetramethylene chain being strung between the two rings. All the N to O distances range from 2·9 to 3·1 Å, suggesting that direct $N^+\cdots:\ddot{O}$ interactions are involved in stabilizing the host–guest complex. Molecular conformation and dimensions, and the geometry of the intermolecular binding are described in detail.

Introduction

The crystal structure of a complex of the semi-rigid system (I) containing two convergent polyether rings with the bis(hexafluorophosphate) salt of tetramethylenediamine has been investigated as part of a programme of studies on structural host–guest relationships among organic compounds. Such studies should throw light on the nature of binding interactions which stabilize complexes of polydentate ligands with smaller guest species, and provide evidence for the interplay of binding and repelling forces that control structural recognition between hosts and guests.

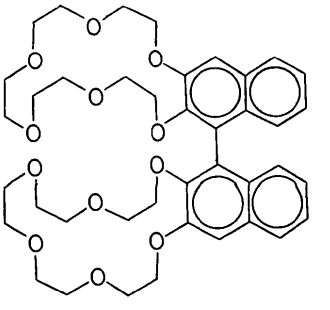

(I)

We have previously described the structures of two model complexes involving ligands with a single macro-ring assembly of binding sites (Goldberg, 1975*a*,*b*).

* Part II: *Acta Cryst.* (1975). B**31**, 2592–2600.

† This work is also a contribution from the Department of Chemistry, University of California at Los Angeles, where a major part of it was carried out.